

## ARTICLE

# Preparation and Characterization of Storage and Emission Functional Material of Cs<sub>2</sub>O-doped 12CaO·7Al<sub>2</sub>O<sub>3</sub>

Shen Ning, Jing Shen, Xing-long Li, Quan-xin Li\*

*Department of Chemical Physics, Lab of Biomass Clean Energy, University of Science and Technology of China, Hefei 230026, China*

(Dated: Received on November 26, 2010; Accepted on December 20, 2010)

We provide a novel approach to generate low-temperature atomic oxygen anions (O<sup>-</sup>) emission using the cesium oxide-doped 12CaO·7Al<sub>2</sub>O<sub>3</sub> (Cs<sub>2</sub>O-doped C12A7). The maximal emission intensity of O<sup>-</sup> from the Cs<sub>2</sub>O-doped C12A7 at 700 °C and 800 V/cm reached about 0.54 μA/cm<sup>2</sup>, which was about two times as strong as that from the un-doped C12A7 (0.23 μA/cm<sup>2</sup>) under the same condition. The initiative temperature of the O<sup>-</sup> emission from the Cs<sub>2</sub>O-doped C12A7 was about 500 °C, which was also much lower than the initiative temperature from the un-doped C12A7 (570 °C) in the given field of 800 V/cm. High pure O<sup>-</sup> emission close to 100% could be obtained from the Cs<sub>2</sub>O-doped C12A7 under the lower temperature (<550 °C). The emission features of the Cs<sub>2</sub>O-doped C12A7, including the emission distribution, temperature effect, and emission branching ratio have been investigated in detail and compared with the un-doped C12A7. The structure and storage characteristics of the resulting material were also investigated via X-ray diffraction and electron paramagnetic resonance. It was found that doping Cs<sub>2</sub>O to C12A7 will lower the initiative emission temperature and enhance the emission intensity.

**Key words:** Atomic oxygen anion, Cs<sub>2</sub>O-doped C12A7, Emission characteristics, Storage characteristics

## I. INTRODUCTION

Atomic oxygen anion (O<sup>-</sup>) is a monovalent negative ion through the attachment of an electron to atomic oxygen, which is one of the most active oxygen species. As one of the important chemical intermediates, atomic oxygen anion is potentially useful in many fields such as chemical synthesis, air cleaning, and surface sterilization [1, 2]. It has been found that anion implantation or deposition into insulated material surfaces is more suitable than the use of positive implantation because anions have negative polarity and low electron affinity, and besides, there are negligible “surface charging-up” in the former [3–5]. Anions have also been used as an alternative to positive ions for ion fusion drivers in inertial confinement fusion because electron accumulation would be prevented [6].

The conventional method to form anions is through the attachment of a free low-energy electron to atom or through anion-molecule reactions, appearing in the processes such as plasma, electron impact, or laser irradiation *etc.* Anions generated in above processes, in general, are complicated and always accompanied by the formation of manifold species. Alternately, we have

developed an approach to selectively generate anions of O<sup>-</sup>, H<sup>-</sup>, F<sup>-</sup>, Cl<sup>-</sup>, and OH<sup>-</sup> via the synthesized anionic storage-emission materials [7–17]. For example, the microporous material of C12A7-O<sup>-</sup> can store and emit O<sup>-</sup>, prepared by the solid-state reaction of CaCO<sub>3</sub> and γ-Al<sub>2</sub>O<sub>3</sub> in the dry oxygen environment [7–10, 18]. The structure of C12A7-O<sup>-</sup> is characterized by a positive charged lattice framework [Ca<sub>24</sub>Al<sub>28</sub>O<sub>64</sub>]<sup>4+</sup> including 12 sub-nanometer sized cages with a free space of about 0.4 nm in diameter [18, 19]. The storage features of O<sup>-</sup> in the cage of C12A7-O<sup>-</sup> have been investigated by the electron paramagnetic resonance (EPR) method [18]. On the other hand, the O<sup>-</sup> anions stored in C12A7-O<sup>-</sup> can be emitted into the gas phase by heating the material [7–10]. The emitted species from the C12A7-O<sup>-</sup> surface are dominated by O<sup>-</sup>. More recently, we have also synthesized various derivatives (*e.g.*, C12A7-OH<sup>-</sup> [11, 12], C12A7-H<sup>-</sup> [13, 14], C12A7-F<sup>-</sup> [15, 16], and C12A7-Cl<sup>-</sup> [17]) and found that these materials or the modified ones would be potentially used in a one-step synthesis of phenol from benzene [20], the reduction of NO [21], a fast microorganisms inactivation [22, 23], the dissociation and oxidation of oxygenated organic compounds [24–26].

Although there have been previous studies on C12A7 and its various derivatives, higher operation temperature remains a main challenge when these materials are used in the anions emission source, catalytic re-

\* Author to whom correspondence should be addressed. E-mail: liqx@ustc.edu.cn

actions, filming modifications and anionic sterilization processes. The present study provides a novel approach to generate low-temperature atomic oxygen anions ( $O^-$ ) emission by using the  $Cs_2O$ -doped  $12CaO \cdot 7Al_2O_3$  ( $Cs_2O$ -doped C12A7). The emission and structure features of the  $Cs_2O$ -doped C12A7 have been investigated in detail. Lower operation temperature, potentially, will promote the practical application of the anion storage-emission material in the  $O^-$  source, chemical synthesis, air cleaning, and surface sterilization.

## II. EXPERIMENTS

### A. Sample preparation

The  $Cs_2O$ -doped C12A7 particles were prepared by the citric acid sol-gel combustion method. All reagents were of analytical grade without further purification. First, appropriate amounts of  $Ca(NO_3)_2 \cdot 4H_2O$ ,  $Al(NO_3)_3 \cdot 9H_2O$ ,  $Cs_2O$ , and polyethylene glycol were dissolved in  $CO(NH_2)_2$  solution (20% in distilled water) with a mass ratio of  $Ca(NO_3)_2 \cdot 4H_2O : Al(NO_3)_3 \cdot 9H_2O : Cs_2O : CO(NH_2)_2 = 11.3354 : 21.0081 : 1.3867 : 12.4800$ . The solution was mixed and stirred at 70 °C for 3 h and formed a transparent solution. Second, ethylene glycol (EG) was added to the above-mentioned solution with a 4:1 molar ratio of EG to CA. The solution was sequentially stirred at 80 °C for 3 h, which led to a sol. The sol was aged at 90 °C for 24 h to form a xerogel. Third, the xerogel was pretreated in air at 250 °C for 1 h to form a precursor powder sample, through a self-combustion process. Finally, the precursor sample was further sintered at 1200 °C in  $O_2$  for 10 h, cooled to room temperature, and finally formed the powder sample of  $Cs_2O$ -doped C12A7. The appropriate  $Cs_2O$  content added to C12A7 was about 12%.

### B. Characterizations of samples

X-ray diffraction (XRD) measurements were carried out to investigate the structure of the prepared samples. The synthesized samples were crushed into particles with the average diameter of 20–30  $\mu m$ . The powder XRD patterns were recorded on an X'pert Pro Philips diffractometer with a  $Cu K\alpha 1$  source ( $\lambda = 1.540598 \text{ \AA}$ ). The measurement was in the  $2\theta$  range of  $10^\circ - 80^\circ$ , step counting time of 5 s, and step size of  $0.017^\circ$  at 298 K. The measurement of the lattice constant was made from diffractometer traces using Si as the internal standard.

EPR measurement was performed to investigate the anionic species (*e.g.*,  $O^-$  and  $O_2^-$ ) in the  $Cs_2O$ -doped C12A7 and un-doped C12A7 bulks. The experiment was conducted at ca 9.1 GHz (X-band) using a JES-FA200 spectrometer at 120 K. Spin concentrations were determined from the second integral of the spectrum using  $CuSO_4 \cdot 5H_2O$  as a standard with an error of about

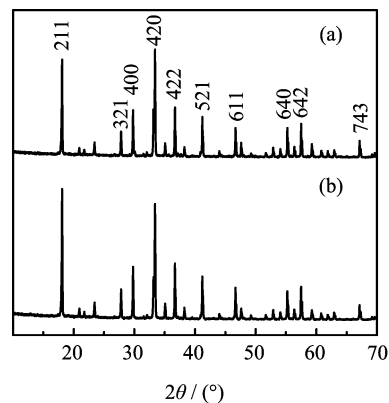


FIG. 1 XRD patterns from (a) un-doped C12A7 and (b)  $Cs_2O$ -doped C12A7.

20%.

The emitted anions from the  $Cs_2O$ -doped C12A7 surface were mass-analyzed by time-of-flight (TOF) mass spectroscopy, and the detailed conditions are the same as the previous study [9–14].

## III. RESULTS AND DISCUSSION

### A. Characterizations and storage characteristics of $Cs_2O$ -doped C12A7 and un-doped C12A7

Figure 1 shows the XRD patterns of the un-doped C12A7 and  $Cs_2O$ -doped C12A7. Through the comparison of the measured peak positions and intensities of the XRD patterns with the standard data in the PDF-09-0413 card, the XRD structure for the present  $Cs_2O$ -doped material completely accords with that of the crystal  $12CaO \cdot 7Al_2O_3$  (C12A7), belonging to  $I\bar{4}3d$  space group [27]. No other phases such as  $Ca_5Al_6O_{14}$  (C5A3),  $Ca_3Al_2O_6$  (C3A), and  $CaAl_2O_4$  (CA) were observed. Thus, the doping process did not destroy the crystal structure of C12A7. The unit cell value derived from twenty stronger diffraction peaks of the  $Cs_2O$ -doped C12A7 was about  $1.195 \pm 0.002 \text{ nm}$ , which agreed very well with the data of the un-doped C12A7  $1.199 \pm 0.001 \text{ nm}$ . All of the diffraction peaks observed from the used  $Cs_2O$ -doped C12A7 sample agreed very well with those from the original ones.

The EPR measurements were performed to investigate the oxygen-containing species such as  $O^-$  and  $O_2^-$  in the resulting material. Figure 2 shows the EPR spectra of the samples mentioned above. The EPR spectra can be decomposed into two components, which are attributed to the anionic oxygen species of  $O^-$  ( $g_{xx} = g_{yy} = 2.036$  and  $g_{zz} = 1.994$ ) and  $O_2^-$  ( $g_{xx} = 2.001$ ,  $g_{yy} = 2.008$ , and  $g_{zz} = 2.074$ ) [11, 17]. The spectral intensity for the  $Cs_2O$ -doped C12A7 was almost the same with that for the un-doped C12A7. By the simulation of the EPR spectra and using  $CuSO_4 \cdot 5H_2O$  as a spin concentrations standard, the

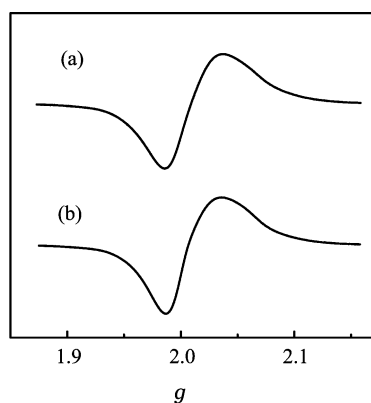


FIG. 2 EPR spectra from (a) un-doped C12A7 and (b) Cs<sub>2</sub>O-doped C12A7.

oxygen species concentrations in the resulting material could be estimated. The concentrations of O<sup>-</sup> and O<sub>2</sub><sup>-</sup> in Cs<sub>2</sub>O-doped C12A7, by simulating the measured EPR spectra, were both about  $(1.2 \pm 0.2) \times 10^{20}$  and  $(1.0 \pm 0.2) \times 10^{20} \text{ cm}^{-3}$  respectively, which were close to the data in the un-doped C12A7 ( $[\text{O}^-] = (1.3 \pm 0.3) \times 10^{20}$  and  $[\text{O}_2^-] = (1.2 \pm 0.2) \times 10^{20} \text{ cm}^{-3}$ ). Accordingly, the chemical formula of the Cs<sub>2</sub>O-doped C12A7 was approximately described as  $[\text{Ca}_{24}\text{Al}_{28}\text{O}_{64}]^{4+} \cdot (\text{O}^-)_{0.2}(\text{O}_2^-)_{0.2}(\text{O}^{2-})_{1.8}$ .

## B. TOF measurements and emission characteristics

The anions emitted from the Cs<sub>2</sub>O-doped C12A7 and un-doped C12A7 surfaces were identified by TOF mass spectroscopy. Figure 3(a) shows typical anionic TOF mass spectra from the Cs<sub>2</sub>O-doped C12A7 at 650 °C under an extraction field of 800 V/cm. At 650 °C, two peaks at  $m/z=0$  and 16 appeared synchronously, which corresponded respectively to the emission of the electrons and O<sup>-</sup> (Fig.3(a)). This indicated that the anionic species emitted from the Cs<sub>2</sub>O-doped C12A7 surface consisted of the O<sup>-</sup> anions and some amount of electrons in this work. It was also noticed that the emission intensity of O<sup>-</sup> from Cs<sub>2</sub>O-doped C12A7 at 650 °C (Fig.3(a)) was almost the same as that from the un-doped C12A7 at 700 °C (Fig.3(b)), indicating that the required emission temperature of O<sup>-</sup> from C12A7 was reduced by doping Cs<sub>2</sub>O.

Figure 4 shows that the emission intensities of O<sup>-</sup> and e<sup>-</sup> from the Cs<sub>2</sub>O-doped C12A7 and un-doped C12A7 as a function of temperature under an applied extraction field of 800 V/cm. The emission intensities of O<sup>-</sup> and e<sup>-</sup> are very sensitive to the surface temperature. The intensity of O<sup>-</sup> from the Cs<sub>2</sub>O-doped C12A7 was about 0.02 μA/cm<sup>2</sup> at 550 °C, and remarkably increased to 0.54 μA/cm<sup>2</sup> at 700 °C. For the un-doped C12A7, however, the intensity of O<sup>-</sup> was 0 at 550 °C in this work and increased to 0.23 μA/cm<sup>2</sup> at 700 °C.

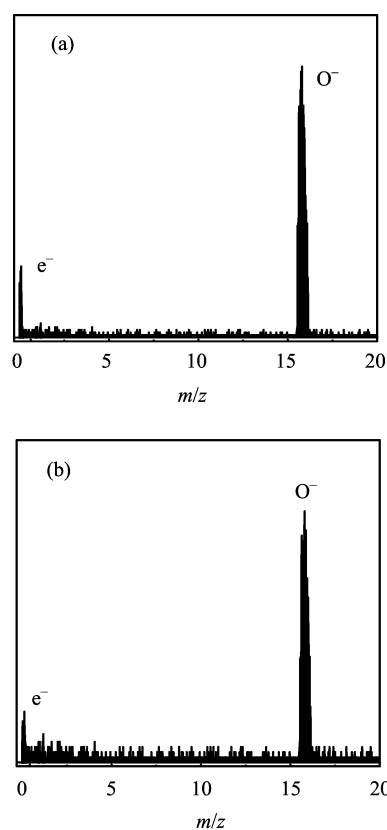


FIG. 3 Typical TOF mass spectra from the material surfaces measured at the extraction field of 800 V/cm. (a) Cs<sub>2</sub>O-doped C12A7 at 650 °C and (b) un-doped C12A7 at 700 °C.

Under the same experimental conditions, the intensity of O<sup>-</sup> from the Cs<sub>2</sub>O-doped C12A7 was significantly stronger than that from un-doped C12A7. This indicated that adding a small amount of Cs<sub>2</sub>O to C12A7 could promote the emission of O<sup>-</sup> and lower the initiative emission temperature from the material surface. In addition, similar temperature effects on the emission intensities of e<sup>-</sup> from the Cs<sub>2</sub>O-doped C12A7 and un-doped C12A7 surfaces were also observed. Moreover, Fig.5 presents the dependence of the emission branching ratio  $r(\text{X}^-)$  ( $\text{X}^- = \text{O}^-$  or e<sup>-</sup>) on temperature at a given applied extraction field of 800 V/cm, which was defined as the intensity ratio of the emission intensity of X<sup>-</sup> to the total emission intensity. For the Cs<sub>2</sub>O-doped C12A7, the emission branching ratio of O<sup>-</sup> was near one below 550 °C and gradually decreased to 71% when the surface temperature increased to 700 °C. The emission branching ratio of e<sup>-</sup> was close to zero at temperatures lower than 550 °C and increased to about 29% at 700 °C. The above results showed that the O<sup>-</sup> were the dominant anionic species emitted from the Cs<sub>2</sub>O-doped C12A7 in the low temperature region. For the un-doped C12A7, the emission branching ratio of O<sup>-</sup> was about 96% at 600 °C and gradually decreased to 92%

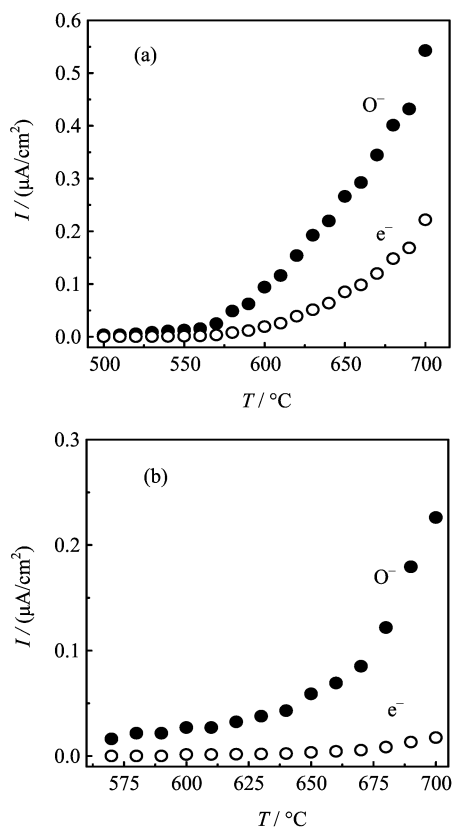


FIG. 4 Effects of temperature on the emission intensities of the  $O^-$  anions and electrons at the extraction field of 800 V/cm. (a)  $Cs_2O$ -doped C12A7, (b) un-doped C12A7.

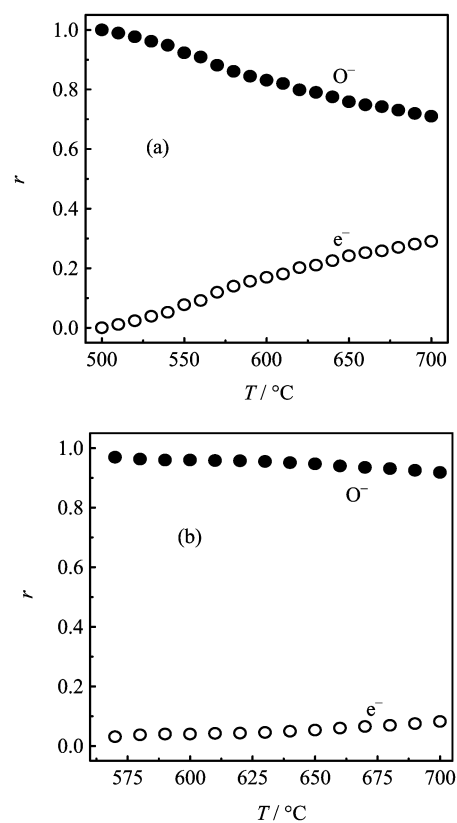


FIG. 5 Emission branching ratios  $r$  of  $O^-$  and  $e^-$  as a function of temperature at the extraction field of 800 V/cm. (a)  $Cs_2O$ -doped C12A7, (b) un-doped C12A7.

at 700 °C. In the high-temperature region ( $>600$  °C), the electrons emission from the  $Cs_2O$ -doped C12A7 was obviously larger than that from the un-doped C12A7.

### C. Formation and emission mechanism of anions for $Cs_2O$ -doped C12A7

Although the  $Cs_2O$ -doped C12A7 had the same positively charged lattice framework structure and possessed a similar anions storage character to that of the un-doped C12A7, the behaviors of the anions emission  $Cs_2O$ -doped C12A7 were rather different from those from the un-doped C12A7. The present results showed that doping a small amount of  $Cs_2O$  to C12A7 could significantly promote the anions emission and lower the initiative emission temperature (Fig.3 and Fig.4). The emission branching ratio of the  $O^-$  anions for the  $Cs_2O$ -doped C12A7 was also different from that for the un-doped C12A7 (Fig.5). The cesium element has a low ionization potential of 3.8 eV and its work function is about 1.8 eV [28].  $Cs_2O$  and such Cs-containing compounds, are usually used as photoelectric material for the micro channel plate (MCP) and photo multiplier tube (PMT) *etc.*, because these Cs-containing mate-

rials possess very high quantum efficiency and effective secondary-electrons emission [30–33]. The reduced initiative emission temperature and enhanced  $O^-$  and  $e^-$  emissions from  $Cs_2O$ -doped C12A7 would be attributed to the promotion effect of  $Cs_2O$  (Fig.3 and Fig.4). The enhancement of the electrons emission from the  $Cs_2O$ -doped C12A7 in the high temperature range may originate from the thermal electrons emission of  $Cs_2O$ . Firstly, it was found that the emission intensity was very sensitive to the surface temperature. The influence of temperature on the anion emission could be qualitatively understood as follows. The  $O^-$  emission from the material surface would mainly be controlled by two kinetic processes, *i.e.*, the diffusion of the  $O^-$  anions from the bulk onto the material surface ( $O^-$  (cages) $\rightarrow O^-$  (surface)), and desorption step from the surface into the gas-phase ( $O^-$  (surface) $\rightarrow O^-$  (gas-phase)). The anions desorption from the surface into the gas-phase was recognized as an endothermic process because anions desorbed from a surface into the gas-phase should overcome the surface barrier when they left the surface [28]. Higher surface temperature was in favor of desorption of  $O^-$  from the surface. Meanwhile, the content of the  $O^-$  anions on the material surface may also increase with the increasing temperature be-

cause higher temperature would promote the diffusion of the charge carriers in C12A7 bulk. On the other hand, we also noticed that the melting point of Cs<sub>2</sub>O was about 490 °C, which meant that the conductivity of C12A7 bulk would be greatly increased after Cs<sub>2</sub>O crystal metaling into ion state in high temperature region (>500 °C). Increased conductivity may also promote the diffusion of charge carriers (O<sup>-</sup> (cages)→O<sup>-</sup> (surface)) in C12A7 bulk as well as electrons.

#### IV. CONCLUSION

By using the cesium oxide-doped 12CaO·7Al<sub>2</sub>O<sub>3</sub> (Cs<sub>2</sub>O-doped C12A7), a novel approach to generate low-temperature atomic oxygen anions (O<sup>-</sup>) emission in the gas-phase has been developed. The synthesized Cs<sub>2</sub>O-doped C12A7, having the cage structure, stored atomic oxygen anions with the concentration about  $(1.2\pm 0.2)\times 10^{20}$  cm<sup>-3</sup>. The emission intensity of O<sup>-</sup> from the Cs<sub>2</sub>O-doped C12A7 at 700 °C and 800 V/cm reached about 0.54 μA/cm<sup>2</sup>, and the initiative temperature of the O<sup>-</sup> emission was about 500 °C. High pure O<sup>-</sup> emission close to 100% could be obtained from the Cs<sub>2</sub>O-doped C12A7 under lower temperature (<550 °C). According to the comparison of characteristics between the Cs<sub>2</sub>O-doped C12A7 and un-doped C12A7, doping Cs<sub>2</sub>O to C12A7 could significantly promote the emission of O<sup>-</sup> and lower the initiative emission temperature from the material surface, which could be attributed to the promotion of the diffusion of charge carriers in C12A7 bulk.

#### V. ACKNOWLEDGMENTS

This work is supported by the National Natural Science Foundation of China (No.50772107), the National High Tech Research and Development Program (No.2009AA05Z435), and the National Basic Research Program of the Ministry of Science and Technology of China (No.2007CB210206).

- [1] J. Lee and J. J. Grabowski, *Chem. Rev.* **92**, 1611 (1992).
- [2] L. Fan, J. Song, P. D. Hildebrand, and C. F. Forney, *J. Appl. Microb.* **93**, 144 (2002).
- [3] T. Shibayama, H. Shindo, and Y. Horiike, *Plasma Sources Sci. Technol.* **5**, 254 (1996).
- [4] H. Shindo, Y. Sawa, and Y. Horiike, *Jpn. J. Appl. Phys.* **34**, L925 (1995).
- [5] J. P. Booth, C. S. Corr, G. A. Curley, J. Jolly, J. Guillon, and T. Földes, *Appl. Phys. Lett.* **88**, 151502 (2006).
- [6] J. Ishikawa, *Rev. Sci. Instrum.* **71**, 1036 (2000).
- [7] Q. X. Li, Y. Torimoto, and M. Sadakata, Patent No.WO/2005/115913.
- [8] Q. X. Li, Y. Torimoto, and M. Sadakata, Japan Patent No.JP2004-160374.
- [9] Q. X. Li, K. Hayashi, M. Nishioka, H. Kashiwagi, M. Hirano, Y. Torimoto, H. Hosono, and M. Sadakata, *Appl. Phys. Lett.* **80**, 4259 (2002).
- [10] Q. X. Li, H. Hosono, M. Hirano, K. Hayashi, M. Nishioka, H. Kashiwagi, Y. Torimoto, and M. Sadakata, *Surf. Sci.* **527**, 100 (2003).
- [11] J. Li, F. Huang, L. Wang, S. Q. Yu, Y. Torimoto, M. Sadakata, and Q. X. Li, *Chem. Mater.* **17**, 2771 (2005).
- [12] J. Li, F. Huang, L. Wang, Z. X. Wang, S. Q. Yu, Y. Torimoto, M. Sadakata, and Q. X. Li, *J. Phys. Chem. B* **109**, 14599 (2005).
- [13] F. Huang, J. Li, H. Xian, J. Tu, J. Q. Sun, S. Q. Yu, Q. X. Li, Y. Torimoto, and M. Sadakata, *Appl. Phys. Lett.* **86**, 114101 (2005).
- [14] F. Huang, J. Li, L. Wang, T. Dong, J. Tu, Y. Torimoto, M. Sadakata, and Q. X. Li, *J. Phys. Chem. B* **109**, 12032 (2005).
- [15] C. F. Song, J. Q. Sun, S. B. Qiu, L. X. Yuan, J. Tu, and Y. F. Torimoto, *Chem. Mater.* **20**, 3473 (2008).
- [16] C. F. Song, J. Q. Sun, J. Li, S. Ning, M. Yamamoto, J. Tu, Y. Torimoto, and Q. X. Li, *J. Phys. Chem. C* **112**, 19061 (2008).
- [17] J. Q. Sun, C. F. Song, S. Ning, S. B. Lin, and Q. X. Li, *Chin. J. Chem. Phys.* **22**, 417 (2009).
- [18] K. Hayashi, M. Hirano, S. Matsuishi, and H. Hosono, *J. Am. Chem. Soc.* **124**, 738 (2002).
- [19] H. B. Bartl and T. Scheller, *Neues Jahrb Mineral Monatsh* **35**, 547 (1970).
- [20] T. Dong, J. Li, F. Huang, L. Wang, J. Tu, Y. Torimoto, M. Sadakata, and Q. X. Li, *Chem. Commun.* 2724 (2005).
- [21] A. M. Gao, X. F. Zhu, H. J. Wang, J. Tu, P. Y. Lin, Y. Torimoto, M. Sadakata, and Q. X. Li, *J. Phys. Chem. B* **110**, 11854 (2006).
- [22] L. Wang, L. Gong, E. Zhao, Z. Yu, Y. Torimoto, M. Sadakata, and Q. X. Li, *Lett. Appl. Microbiol.* **45**, 200 (2007).
- [23] L. C. Li, L. Wang, Z. Yu, X. Z. Lv, and Q. X. Li, *Plasma Sources Sci. Technol.* **9**, 119 (2007).
- [24] Z. X. Wang, Y. Pan, T. Dong, X. F. Zhu, T. Kan, L. X. Yuan, Y. Torimoto, M. Sadakata, and Q. X. Li, *Appl. Catal. A* **320**, 24 (2007).
- [25] T. Dong, Z. X. Wang, L. X. Yuan, Y. Torimoto, M. Sadakata, and Q. X. Li, *Catal. Lett.* **119**, 29 (2007).
- [26] Z. X. Wang, T. Dong, L. X. Yuan, T. Kan, X. F. Zhu, Y. Torimoto, M. Sadakata, and Q. X. Li, *Energy Fuels* **21**, 2421 (2007).
- [27] J. Jeevaratnam, F. P. Glasser, and L. S. D. Glasser, *J. Am. Ceram. Soc.* **47**, 105 (1964).
- [28] B. Raton, *Handbook of Chemistry and Physics*, 64th Edn., New York: CRC Press, (1983).
- [29] G. A. Somorjai, *Introduction to Surface Chemistry and Catalysis*, New York: John Wiley and Sons, 381 (1994).
- [30] R. Hemphill and J. Edelstein, *Appl. Opt.* **42**, 2251 (2003).
- [31] Steve Mitchell, University of Colorado at Boulder, ECEN 5645 Spring (2008).
- [32] S. Gemming, G. Seifert, C. Mühle, M. Jansen, A. Albu-Yaron, T. Arad, and R. Tenne, *J. Solid State Chem.* **178**, 1190 (2005).
- [33] T. J. Vink, A. R. Balkenende, R. G. F. A. Verbeek, H. A. M. van Hal, and S. T. de Zwart, *Appl. Phys. Lett.* **80**, 2216 (2002).